

Measurement of the Prompt D^0 Nuclear Modification Factor in p -Pb Collisions at $\sqrt{s_{NN}} = 8.16$ TeV

R. Aaij *et al.**
(LHCb Collaboration)

 (Received 16 May 2022; accepted 24 February 2023; published 6 September 2023)

The production of prompt D^0 mesons in proton-lead collisions in both the forward and backward rapidity regions at a center-of-mass energy per nucleon pair of $\sqrt{s_{NN}} = 8.16$ TeV is measured by the LHCb experiment. The nuclear modification factor of prompt D^0 mesons is determined as a function of the transverse momentum p_T , and the rapidity in the nucleon-nucleon center-of-mass frame y^* . In the forward rapidity region, significantly suppressed production with respect to pp collisions is measured, which provides significant constraints on models of nuclear parton distributions and hadron production down to the very low Bjorken- x region of $\sim 10^{-5}$. In the backward rapidity region, a suppression with a significance of 2.0–3.8 standard deviations compared to parton distribution functions in a nuclear environment expectations is found in the kinematic region of $p_T > 6$ GeV/ c and $-3.25 < y^* < -2.5$, corresponding to $x \sim 0.01$.

DOI: [10.1103/PhysRevLett.131.102301](https://doi.org/10.1103/PhysRevLett.131.102301)

Charm and beauty quarks are produced in the early stage of ultrarelativistic heavy-ion collisions and are strongly affected by the presence of deconfined hot nuclear matter, known as quark-gluon plasma (QGP) [1], as well as by cold nuclear matter (CNM) effects. The latter can be studied in proton-nucleus collisions where QGP effects are not expected to be dominant. Heavy-flavor hadrons, i.e., hadrons containing one or more heavy quark, are affected by CNM effects at all stages of their production. At LHC energies, the most relevant effect is from the initial state, where the parton distribution functions in a nuclear environment (NPDF) [2–4] differ from those in isolated nucleons at all values of Bjorken momentum fraction x . Parton density decreases at $x \lesssim 0.1$ due to nuclear shadowing, and increases at $0.1 \lesssim x \lesssim 0.3$ as a result of antishadowing [5]. Therefore different effects are expected to be relevant at different intervals of rapidity, which is strongly correlated with x . The parton distributions at small x can also be described by the color-glass condensate effective theory (CGC) as a saturated gluonic system [6]. Moreover, multiple scattering and energy loss may occur when the incoming partons and the heavy quarks traverse the nuclear medium [7–9]. Other initial-state or even final-state effects [10,11] may also modify the kinematic distributions of produced heavy-flavor hadrons, as suggested

by their surprisingly large spatial anisotropy in momentum in high-multiplicity p -Pb collisions [12,13].

The LHCb Collaboration has recently measured the production cross section of various heavy-flavor hadrons in p -Pb collisions at forward rapidity, including the production of prompt D^0 and Λ_c^+ hadrons at a center-of-mass energy per nucleon pair of $\sqrt{s_{NN}} = 5.02$ TeV [14,15], and the production of J/ψ , B^0 , B^+ , Λ_b^0 and $\Upsilon(nS)$ states at $\sqrt{s_{NN}} = 8.16$ TeV [16–18]. The ALICE collaboration has measured open charm production at midrapidity at $\sqrt{s_{NN}} = 5.02$ TeV [19–24]. Other measurements of heavy-flavor production in p -Pb collisions at the LHC are also reported [25–36]. CNM effects have also been investigated with heavy-quark production at the RHIC collider in d Au collisions at $\sqrt{s_{NN}} = 200$ GeV [37,38]. These measurements have led to significantly reduced uncertainties of NPDFs in the small- x region [39,40], especially with the constraints from the LHCb D^0 measurements at $\sqrt{s_{NN}} = 5.02$ TeV [14].

This Letter reports the measurement of the production cross section and the nuclear modification factor R_{pPb} of prompt D^0 mesons in p -Pb collisions at $\sqrt{s_{NN}} = 8.16$ TeV performed with the LHCb detector [41]. The quantity R_{pPb} is defined as the ratio of the cross section in p -Pb collisions to the corresponding cross section in pp collisions scaled by the mass number of Pb. Prompt mesons are those directly produced in proton-lead collisions or from strong decays of excited charm hadrons, rather than from decays of beauty hadrons. This measurement uses a data sample 20 times larger than that used for the LHCb D^0 measurements at $\sqrt{s_{NN}} = 5.02$ TeV [14]. The results can be incorporated into global fits together with all other relevant

*Full author list given at the end of the Letter.

Published by the American Physical Society under the terms of the [Creative Commons Attribution 4.0 International license](https://creativecommons.org/licenses/by/4.0/). Further distribution of this work must maintain attribution to the author(s) and the published article's title, journal citation, and DOI.

measurements to improve NPDF parametrizations and to test other possible CNM effects.

The LHCb detector is a single-arm forward spectrometer designed for studying heavy-flavor particles, described in detail in Refs. [41,42]. The data sample for this analysis consists of p -Pb collisions collected with the LHCb detector at the end of 2016, including two different configurations: forward collisions (p beam coming from upstream of the vertex detector) and backward collisions (p beam coming from downstream of the vertex detector), corresponding to an integrated luminosity of $12.2 \pm 0.3 \text{ nb}^{-1}$ ($18.6 \pm 0.5 \text{ nb}^{-1}$) for forward (backward) collisions [17,43]. The forward (backward) configuration data cover a positive (negative) rapidity range of $1.5 < y^* < 4.0$ ($-5.0 < y^* < -2.5$), corresponding to an x coverage of approximately 10^{-5} – 10^{-3} (10^{-2} – 10^{-1}) for the partons of the Pb nucleus, with the positive z axis defined as the direction of the proton beam.

Simulation samples are required to model the effects of the detector acceptance and the selection requirements. The D^0 mesons are generated using PYTHIA 8 [44] with a specific LHCb configuration [45] and embedded into minimum-bias p -Pb events from the EPOS-LHC generator [46]. Decays of unstable particles are described by EvtGen [47], in which final-state radiation is generated using PHOTOS [48]. The interaction of the generated particles with the detector, and its response, are implemented using the GEANT4 toolkit [49] as described in Ref. [50].

The double differential cross section for prompt D^0 production is measured as a function of y^* , the rapidity in the nucleon-nucleon center-of-mass frame, and p_T , the transverse momentum with respect to the beam direction. The quantity y^* is related to the rapidity in the laboratory frame y_{lab} by $y^* = y_{\text{lab}} - 0.465$ for p -Pb collisions. The differential cross section in a given (p_T, y^*) interval is defined as

$$\frac{d^2\sigma}{dp_T dy^*} \equiv \frac{N(D^0 \rightarrow K^\mp \pi^\pm) + N(\bar{D}^0 \rightarrow K^\pm \pi^\mp)}{\mathcal{L} \times \epsilon_{\text{tot}} \times \mathcal{B}(D^0 \rightarrow K^\mp \pi^\pm) \times \Delta p_T \times \Delta y^*}, \quad (1)$$

where $N(D^0 \rightarrow K^\mp \pi^\pm)$ and $N(\bar{D}^0 \rightarrow K^\pm \pi^\mp)$ are the D^0 and \bar{D}^0 signal yields, \mathcal{L} is the integrated luminosity, ϵ_{tot} is the total efficiency, $\mathcal{B}(D^0 \rightarrow K^\mp \pi^\pm) = (3.96 \pm 0.03)\%$ is the sum of branching fractions for the decays $D^0 \rightarrow K^- \pi^+$ and $D^0 \rightarrow K^+ \pi^-$ [51], and Δp_T and Δy^* are the p_T and y^* interval widths. The D^0 mesons are reconstructed through the $D^0 \rightarrow K^- \pi^+$ and the doubly Cabibbo-suppressed $D^0 \rightarrow K^+ \pi^-$ decay channels and their charge conjugates. (The branching fraction of $D^0 \rightarrow K^+ \pi^-$ channel is 2 orders of magnitude smaller than that of $D^0 \rightarrow K^- \pi^+$.) The measurement is performed within a p_T range of $0 < p_T < 30 \text{ GeV}/c$, and the rapidity range defined above. Throughout the analysis, the measurements are for the combined sample of D^0 and \bar{D}^0 mesons. The signal yields

and the total efficiency are determined in each kinematic interval.

The D^0 candidates are built from K^\mp and π^\pm candidate tracks. The selection criteria are similar to those used in D^0 production measurements in p -Pb collisions at $\sqrt{s_{NN}} = 5.02 \text{ TeV}$ [14]. The reconstructed K^\mp and π^\pm tracks are required to have transverse momentum greater than $0.4 \text{ GeV}/c$. Both tracks are also required to be of good quality, come from a common vertex, and pass particle identification (PID) requirements.

The inclusive D^0 signal yield is the sum of the prompt D^0 mesons and those produced in the decays of b hadrons, denoted “*from b*.” This inclusive yield is determined using an extended unbinned maximum-likelihood fit to the distribution of the $K \pi$ invariant mass, $M(K\pi)$. The $M(K\pi)$ distribution of the signal is described by a sum of a Crystal Ball function [52] and a Gaussian function sharing a common mean value, while the background shape is described by a linear function, following the measurement of Ref. [14]. The prompt signal yield is determined by fitting the distribution of $\log_{10}(\chi_{\text{IP}}^2)$ of the D^0 candidates, where χ_{IP}^2 is defined as the difference in the vertex fit χ^2 of a given primary vertex reconstructed with and without the D^0 candidate under consideration. The background component in the $\log_{10}(\chi_{\text{IP}}^2)$ distribution is subtracted using the *sPlot* technique [53] with $M(K\pi)$ as the discriminating variable. The shapes of the $\log_{10}(\chi_{\text{IP}}^2)$ distribution corresponding to the prompt and *from-b* components are described independently by Bukin functions [54], which are asymmetric functions with tails described by Gaussian functions. The parameters of the functions describing the prompt and *from-b* components are fixed to those from simulation. The invariant-mass and $\log_{10}(\chi_{\text{IP}}^2)$ distributions of the forward and backward samples are given in Supplemental Material [55].

The total efficiency ϵ_{tot} is the product of the geometrical acceptance of the detector, the selection and reconstruction efficiency, the PID efficiency, and the trigger efficiency, with each component determined separately. The geometrical acceptance and the selection, reconstruction, and trigger efficiencies are evaluated with the p -Pb simulation samples. The simulation sample is weighted in order to match the occupancy of the tracking system observed in the data. The track reconstruction efficiency is calibrated with minimum-bias $J/\psi \rightarrow \mu^+ \mu^-$ and $K_S^0 \rightarrow \pi^+ \pi^-$ samples, using the tag-and-probe approach employed in Ref. [56]. The trigger efficiency obtained from the simulation is validated by measuring it from control data samples recorded with minimum trigger requirements. The PID efficiency is estimated with a tag-and-probe method [57,58], using the D^* -tagged decay chain $D^{*+} \rightarrow D^0 \pi^+$ with $D^0 \rightarrow K^- \pi^+$ decays.

Several sources of systematic uncertainty are considered and described in detail in Supplemental Material [55],

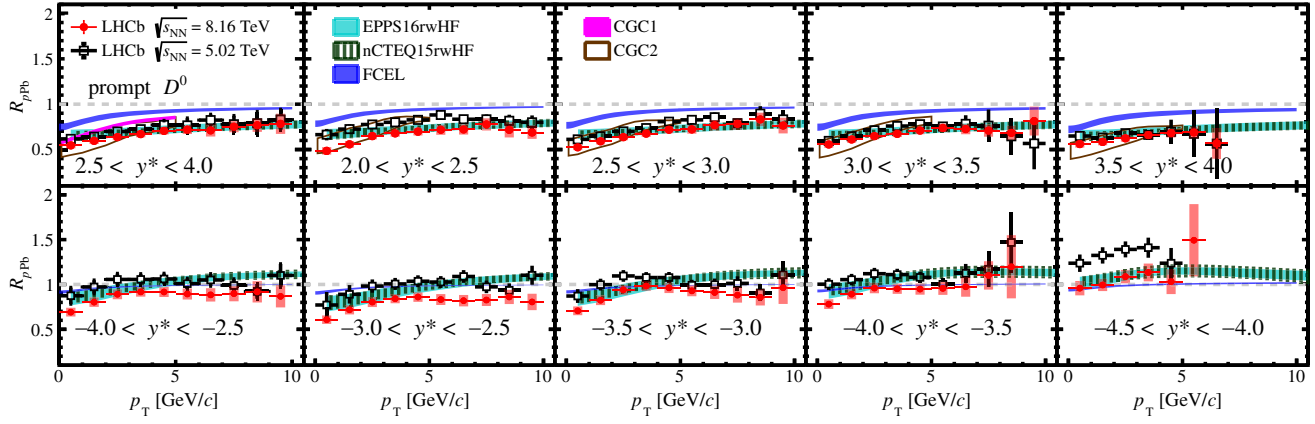


FIG. 1. Nuclear modification factor as a function of p_T in different y^* intervals for prompt D^0 mesons in the (top) forward and (bottom) backward regions. The error bars show the statistical uncertainties and the boxes show the systematic uncertainties. The LHCb results at $\sqrt{s_{NN}} = 5.02$ TeV [14] and theoretical calculations at $\sqrt{s_{NN}} = 8.16$ TeV from Refs. [9,61–64] are also shown. For LHCb results at $\sqrt{s_{NN}} = 5.02$ TeV, the error bars show the quadric sum of statistical and systematic uncertainties.

where results and numerical values for the double-differential cross section are also given. The total prompt D^0 production cross section, obtained by integrating the double-differential measurements, is $297.6 \pm 0.6 \pm 14.0$ mb in the kinematic range of $0 < p_T < 30$ GeV/ c and $1.5 < y^* < 4.0$ for the forward rapidity region, and $315.2 \pm 0.2 \pm 17.8$ mb in the kinematic range of $0 < p_T < 30$ GeV/ c and $-5.0 < y^* < -2.5$ in the backward rapidity region. The first uncertainties are statistical and the second systematic.

The nuclear modification factor R_{pPb} is defined as

$$R_{pPb}(p_T, y^*) \equiv \frac{1}{A} \frac{d^2\sigma_{pPb}(p_T, y^*)/(dp_T dy^*)}{d^2\sigma_{pp}(p_T, y^*)/(dp_T dy^*)}, \quad (2)$$

where $A = 208$ is the mass number of the lead nucleus and σ_{pp} is the prompt D^0 production cross section in pp collisions at $\sqrt{s} = 8.16$ TeV. An interpolation between LHCb measurements at $\sqrt{s} = 5.02$ TeV and $\sqrt{s} = 13$ TeV [59,60] is performed to obtain $d^2\sigma_{pp}(p_T, y^*)/(dp_T dy^*)$, using a power-law function $\sigma(\sqrt{s}) = p_0(\sqrt{s})^{p_1}$. A linear function is also considered. The interpolation uncertainty comprises the difference between the two interpolation models, and the propagated total uncertainties from the pp measurements, and typically amounts to 3% (5%) at forward (backward) rapidity. The interpolation is performed within the common measured kinematic range of $p_T < 10$ GeV/ c and $2.0 < y < 4.5$ for 5.02 and 13 TeV pp results, hence R_{pPb} is measured in that range.

The nuclear modification factor of the D^0 meson as a function of p_T is displayed in Fig. 1, where eight panels report the results in different y^* subintervals of $\Delta y^* = 0.5$ and the two left panels are in the common range between the forward and backward rapidity coverage, $2.5 < |y^*| < 4$. Figures showing R_{pPb} and the forward-backward production ratio R_{FB} as functions of y^* and p_T in $\Delta y^* = 0.25$ intervals, as well as the numerical values are

given in Supplemental Material [55]. A significant suppression of the cross section in p -Pb collisions, with respect to that in pp collisions scaled by the lead mass number, is observed at forward rapidity as well as at backward rapidity up to $y^* \sim -3.5$.

The R_{pPb} results are compared with several theoretical calculations. The HELAC-Onia approach [65,66] is based on a data-driven modeling of the scattering at partonic level folded with the free proton PDFs [67]. The calculations are first tuned by fitting the cross sections measured in pp collisions at the LHC. Then, the modified PDFs of nucleons in the Pb nucleus are introduced in the model to calculate the cross sections in p -Pb collisions and to estimate the effect of NPPDFs, neglecting other cold and hot nuclear matter effects. Reweighted EPPS16 [61] and NCTEQ15 [62] NPPDF sets, where LHC heavy flavor data [14,19–21] are incorporated by performing a Bayesian-reweighting analysis [68], are used in the calculations, resulting in considerably reduced uncertainties than calculations using the default NPPDFs. The uncertainties are dominated by NPPDF parametrizations and correspond to a 68% confidence interval. At forward rapidity, the calculations are in general agreement with the data, except for $p_T < 1$ GeV/ c where the predictions are about 2 standard deviations larger than the data. This discrepancy suggests stronger shadowing or additional energy loss at low x . At backward rapidity, for $p_T > 6$ GeV/ c and $-3.5 < y^* < -2.5$ the data are lower than the calculations by 2.0–3.8 standard deviations, indicating a weaker antishadowing effect or possible final-state effects.

The nuclear modification factor is also compared with two calculations based on the CGC effective field theory, CGC1 and CGC2. Since gluon saturation is expected to occur at small x and Q^2 , the calculations are applicable for $p_T < 5$ GeV/ c at forward rapidity where saturation effects are relevant. For CGC1 [63,69] the D -meson production is calculated with the color dipole formalism, and the optical

Glauber model is used to relate the initial condition of a nucleus to that of the proton. For CGC2 [64] the color dipole approach is combined with a heavy-quark fragmentation function to calculate the cross sections. The CGC1 predictions have much smaller uncertainties than the CGC2 ones, because the CGC1 uncertainties include only variations of the c quark mass and of the factorization scale, which largely cancel out in the $R_{p\text{Pb}}$ ratio versus p_T . CGC1 is consistent with the upper bound of CGC2 and is slightly higher than the data. CGC2 shows a stronger suppression than HELAC-Onia calculations and gives a better description of the data, especially for $p_T < 3 \text{ GeV}/c$.

A fourth calculation estimates D^0 suppression caused by medium-induced fully coherent energy loss (FCEL) [9], a CNM effect where the interference between initial- and final-state gluon radiation results in an energy loss proportional to the incoming parton energy. The FCEL prediction shown in Fig. 1 does not consider the modification of NPDFs. The effect is significant for low p_T , suggesting the suppression observed for $p_T < 1 \text{ GeV}/c$ may be caused by combined effects from NPDFs and FCEL. For $p_T > 6 \text{ GeV}/c$ the suppression due to FCEL is negligible, thus the discrepancy between the data and HELAC-Onia calculations with NPDFs at backward rapidity cannot be attributed to FCEL effects.

The results are also compared with the LHCb D^0 measurement at $\sqrt{s_{NN}} = 5.02 \text{ TeV}$ [14]. At forward rapidity the $R_{p\text{Pb}}$ values at the two energies are compatible, while at backward rapidity the 8.16 TeV data are significantly lower. The difference could be related to the different Bjorken- x coverage at the two collision energies, while effects related to the Pb-going hemisphere other than

NPDFs and FCEL, such as final-state energy loss in a high-particle-density environment, may also show a $\sqrt{s_{NN}}$ dependence as more charged hadrons are produced in 8.16 TeV collisions. On the other hand, the model calculations offer limited insights into collision energy dependence. HELAC-Onia predictions based on NPDFs are compatible between the two $\sqrt{s_{NN}}$ values due to the large uncertainty of the NPDFs used in the 5.02 TeV calculation. The CGC models show similar values at 5.02 and 8.16 TeV at forward rapidity while they are not applicable at backward. Effects due to FCEL are generally small at backward rapidity.

It is essential to study the impact of Bjorken- x coverage in order to interpret the energy dependence observed in the data. However, x and the momentum transfer Q^2 [5] are partonic quantities that cannot be directly measured in hadronic collisions. Instead, experimental proxies x_{exp} and Q_{exp}^2 , defined as

$$x_{\text{exp}} \equiv 2 \frac{\sqrt{p_T^2(D^0) + M^2(D^0)}}{\sqrt{s_{NN}}} e^{-y^*}$$

$$\text{and } Q_{\text{exp}}^2 \equiv p_T^2(D^0) + M^2(D^0), \quad (3)$$

are introduced to approximate the variation of $R_{p\text{Pb}}$ with x and Q^2 , where $M(D^0)$ and $p_T(D^0)$ denote the mass and p_T of D^0 mesons, respectively.

Figure 2 shows $R_{p\text{Pb}}$ as a function of x_{exp} in five Q_{exp}^2 intervals, for D^0 mesons measured in this work at 8.16 TeV, and at 5.02 TeV from Ref. [14]. The x_{exp} coverage of the 8.16 TeV data extends lower than that of the 5.02 TeV

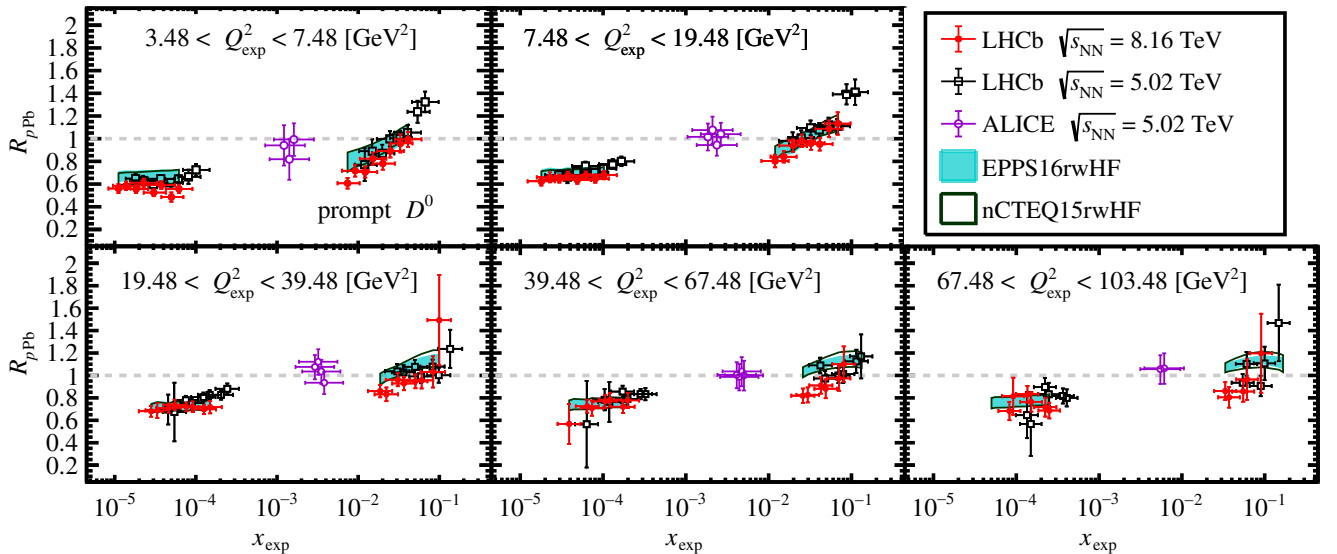


FIG. 2. Nuclear modification factor as a function of x_{exp} in different Q_{exp}^2 intervals for prompt D^0 mesons for LHCb results at $\sqrt{s_{NN}} = 8.16 \text{ TeV}$ and $\sqrt{s_{NN}} = 5.02$ [14] and the ALICE result at $\sqrt{s_{NN}} = 5.02 \text{ TeV}$ [22]. Theoretical calculations at $\sqrt{s_{NN}} = 8.16 \text{ TeV}$ from Refs. [61,62] are also shown. The horizontal error bars account for the maximum and minimum x_{exp} values for a given (p_T, y^*) interval and the vertical error bars show the quadric sum of statistical and systematic uncertainties.

measurements due to the higher $\sqrt{s_{NN}}$ value, reaching down to $x_{\text{exp}} \sim 10^{-5}$ in the interval $3.48 < Q_{\text{exp}}^2 < 7.48 \text{ GeV}^2$, which corresponds to $p_T < 2 \text{ GeV}/c$. The 8.16 TeV data are also more precise. Data from the two energies are in good agreement with each other at common x_{exp} values. The measurements form a consistent trend from the small x_{exp} region corresponding to forward rapidity to the large x_{exp} region corresponding to backward rapidity, for all Q_{exp}^2 intervals. The $D^0 R_{p\text{Pb}}$ ratio at 5.02 TeV at midrapidity [22] measured by the ALICE Collaboration is also added to Fig. 2, and is compatible with the trend within uncertainties. The trend suggests that the $\sqrt{s_{NN}}$ dependence observed at backward rapidity in Fig. 1 arises from different x coverage in a kinematic region where $R_{p\text{Pb}}$ depends strongly on x .

The HELAC-Onia predictions are also transformed according to Eq. (3) and shown in Fig. 2. In the small x_{exp} region, the calculations are in general agreement with the data, except for the interval $3.48 < Q_{\text{exp}}^2 < 7.48 \text{ GeV}^2$ ($p_T < 2 \text{ GeV}/c$) and $10^{-5} < x_{\text{exp}} < 10^{-4}$, where the NPDF expectations are slightly larger than the data and show greater uncertainty. The data hint at a stronger shadowing effect, or other possible effects such as FCEL, that suppresses low- p_T D^0 production at forward rapidity. Moreover, estimations from Ref. [70] suggest gluon saturation may occur in this region. At backward rapidity, the $R_{p\text{Pb}}$ values from the model are larger than those in the data for $Q_{\text{exp}}^2 > 19.48 \text{ GeV}^2$ ($p_T > 4 \text{ GeV}/c$) and $10^{-2} < x_{\text{exp}} < 10^{-1}$, indicating smaller antishadowing effects in the data if nuclear effects other than NPDFs are negligible. Alternatively, it suggests additional suppression mechanisms, such as final-state energy loss, may occur at backward rapidity.

In summary, the prompt D^0 production cross section is measured at the LHCb experiment in proton-lead collisions at $\sqrt{s_{NN}} = 8.16 \text{ TeV}$, at both forward and backward rapidities. The nuclear modification factors are measured with high accuracy and show strong cold nuclear matter effects. A stronger suppression than the predictions of NPDF calculations is observed for the lowest transverse momentum region of $p_T < 1 \text{ GeV}/c$ at forward rapidity, hinting at a stronger shadowing than predicted at Bjorken- $x \sim 10^{-5}$, or additional effects at play. For the backward rapidity range of $-3.5 < y^* < -2.5$, the $R_{p\text{Pb}}$ values are lower than NPDF calculations at $p_T > 6 \text{ GeV}/c$ with a significance of 2.0–3.8 standard deviations, indicating a weaker antishadowing effect than the model or additional final-state effects at backward rapidity. This Letter presents the most precise measurement of the prompt D^0 production in p -Pb collisions to date, providing unique constraints to improve NPDF parametrization down to $x \sim 10^{-5}$.

We express our gratitude to our colleagues in the CERN accelerator departments for the excellent performance of

the LHC. We thank the technical and administrative staff at the LHCb institutes. We acknowledge support from CERN and from the national agencies: CAPES, CNPq, FAPERJ and FINEP (Brazil); MOST and NSFC (China); CNRS/IN2P3 (France); BMBF, DFG and MPG (Germany); INFN (Italy); NWO (Netherlands); MNiSW and NCN (Poland); MEN/IFA (Romania); MICINN (Spain); SNSF and SER (Switzerland); NASU (Ukraine); STFC (United Kingdom); DOE NP and NSF (USA). We acknowledge the computing resources that are provided by CERN, IN2P3 (France), KIT and DESY (Germany), INFN (Italy), SURF (Netherlands), PIC (Spain), GridPP (United Kingdom), CSCS (Switzerland), IFIN-HH (Romania), CBPF (Brazil), Polish WLCG (Poland) and NERSC (USA). We are indebted to the communities behind the multiple open-source software packages on which we depend. Individual groups or members have received support from ARC and ARDC (Australia); Minciencias (Colombia); AvH Foundation (Germany); EPLANET, Marie Skłodowska-Curie Actions and ERC (European Union); A*MIDEX, ANR, IPhU and Labex P2IO, and Région Auvergne-Rhône-Alpes (France); Key Research Program of Frontier Sciences of CAS, CAS PIFI, CAS CCEPP, Fundamental Research Funds for the Central Universities, and Sci. & Tech. Program of Guangzhou (China); GVA, XuntaGal, GENCAT and Prog. Atracción Talento, CM (Spain); SRC (Sweden); the Leverhulme Trust, the Royal Society and UKRI (United Kingdom).

-
- [1] K. Yagi, T. Hatsuda, and Y. Miake, *Quark-Gluon Plasma: From Big Bang to Little Bang* (Cambridge University Press, Cambridge, England, 2005), Vol. 23.
 - [2] K. J. Eskola, H. Paukkunen, and C. A. Salgado, EPS09: A new generation of NLO and LO nuclear parton distribution functions, *J. High Energy Phys.* **04** (2009) 065.
 - [3] D. de Florian and R. Sassot, Nuclear parton distributions at next-to-leading order, *Phys. Rev. D* **69**, 074028 (2004).
 - [4] M. Hirai, S. Kumano, and T.-H. Nagai, Determination of nuclear parton distribution functions and their uncertainties in next-to-leading order, *Phys. Rev. C* **76**, 065207 (2007).
 - [5] N. Armesto, Nuclear shadowing, *J. Phys. G* **32**, R367 (2006).
 - [6] F. Gelis, E. Iancu, J. Jalilian-Marian, and R. Venugopalan, The color glass condensate, *Annu. Rev. Nucl. Part. Sci.* **60**, 463 (2010).
 - [7] I. Vitev, Non-Abelian energy loss in cold nuclear matter, *Phys. Rev. C* **75**, 064906 (2007).
 - [8] Z.-B. Kang, I. Vitev, E. Wang, H. Xing, and C. Zhang, Multiple scattering effects on heavy meson production in $p + A$ collisions at backward rapidity, *Phys. Lett. B* **740**, 23 (2015).
 - [9] F. Arleo, G. Jackson, and S. Peigné, Impact of fully coherent energy loss on heavy meson production in pA collisions, *J. High Energy Phys.* **01** (2022) 164.

- [10] C. Zhang, C. Marquet, G.-Y. Qin, S.-Y. Wei, and B.-W. Xiao, Elliptic Flow of Heavy Quarkonia in pA Collisions, *Phys. Rev. Lett.* **122**, 172302 (2019).
- [11] W. Zhao, C. M. Ko, Y.-X. Liu, G.-Y. Qin, and H. Song, Probing the Partonic Degrees of Freedom in High-Multiplicity p -Pb collisions at $\sqrt{s_{NN}} = 5.02$ TeV, *Phys. Rev. Lett.* **125**, 072301 (2020).
- [12] A. M. Sirunyan *et al.* (CMS Collaboration), Elliptic Flow of Charm and Strange Hadrons in High-Multiplicity p -Pb Collisions at $\sqrt{s_{NN}} = 8.16$ TeV, *Phys. Rev. Lett.* **121**, 082301 (2018).
- [13] A. M. Sirunyan *et al.* (CMS Collaboration), Observation of prompt J/ψ meson elliptic flow in high-multiplicity p -Pb collisions at $\sqrt{s_{NN}} = 8.16$ TeV, *Phys. Lett. B* **791**, 172 (2019).
- [14] R. Aaij *et al.* (LHCb Collaboration), Study of prompt D^0 meson production in p -Pb collisions at $\sqrt{s_{NN}} = 5$ TeV, *J. High Energy Phys.* **10** (2017) 090.
- [15] R. Aaij *et al.* (LHCb Collaboration), Prompt Λ_c^+ production in p -Pb collisions at $\sqrt{s_{NN}} = 5.02$ TeV, *J. High Energy Phys.* **02** (2019) 102.
- [16] R. Aaij *et al.* (LHCb Collaboration), Prompt and nonprompt J/ψ production and nuclear modification in p -Pb collisions at $\sqrt{s_{NN}} = 8.16$ TeV, *Phys. Lett. B* **774**, 159 (2017).
- [17] R. Aaij *et al.* (LHCb Collaboration), Measurement of B^+ , B^0 , and Λ_b^0 production in p -Pb collisions at $\sqrt{s_{NN}} = 8.16$ TeV, *Phys. Rev. D* **99**, 052011 (2019).
- [18] R. Aaij *et al.* (LHCb Collaboration), Study of Υ production in p -Pb collisions at $\sqrt{s_{NN}} = 8.16$ TeV, *J. High Energy Phys.* **11** (2018) 194.
- [19] B. B. Abelev *et al.* (ALICE Collaboration), Measurement of Prompt D -Meson Production in p -Pb Collisions at $\sqrt{s_{NN}} = 5.02$ TeV, *Phys. Rev. Lett.* **113**, 232301 (2014).
- [20] J. Adam *et al.* (ALICE Collaboration), Measurement of D -meson production versus multiplicity in p -Pb collisions at $\sqrt{s_{NN}} = 5.02$ TeV, *J. High Energy Phys.* **08** (2016) 078.
- [21] J. Adam *et al.* (ALICE Collaboration), D -meson production in p -Pb collisions at $\sqrt{s_{NN}} = 5.02$ TeV and in pp collisions at $\sqrt{s} = 7$ TeV, *Phys. Rev. C* **94**, 054908 (2016).
- [22] S. Acharya *et al.* (ALICE Collaboration), Measurement of prompt D^0 , D^+ , D^{*+} , and D_s^+ production in p -Pb collisions at $\sqrt{s_{NN}} = 5.02$ TeV, *J. High Energy Phys.* **12** (2019) 092.
- [23] S. Acharya *et al.* (ALICE Collaboration), Λ_c^+ Production and Baryon-to-Meson Ratios in pp and p -Pb Collisions at $\sqrt{s_{NN}} = 5.02$ TeV at the LHC, *Phys. Rev. Lett.* **127**, 202301 (2021).
- [24] S. Acharya *et al.* (ALICE Collaboration), Λ_c^+ production in pp and in p -Pb collisions at $\sqrt{s_{NN}} = 5.02$ TeV, *Phys. Rev. C* **104**, 054905 (2021).
- [25] S. Acharya *et al.* (ALICE Collaboration), Production of muons from heavy-flavour hadron decays in p -Pb collisions at $\sqrt{s_{NN}} = 5.02$ TeV, *Phys. Lett. B* **770**, 459 (2017).
- [26] S. Acharya *et al.* (ALICE Collaboration), Measurement of nuclear effects on $\psi(2S)$ production in p -Pb collisions at $\sqrt{s_{NN}} = 8.16$ TeV, *J. High Energy Phys.* **07** (2020) 237.
- [27] S. Acharya *et al.* (ALICE Collaboration), Υ production in p -Pb collisions at $\sqrt{s_{NN}} = 8.16$ TeV, *Phys. Lett. B* **806**, 135486 (2020).
- [28] S. Acharya *et al.* (ALICE Collaboration), Inclusive J/ψ production at forward and backward rapidity in p -Pb collisions at $\sqrt{s_{NN}} = 8.16$ TeV, *J. High Energy Phys.* **07** (2018) 160.
- [29] S. Acharya *et al.* (ALICE Collaboration), Prompt and non-prompt J/ψ production and nuclear modification at mid-rapidity in p -Pb collisions at $\sqrt{s_{NN}} = 5.02$ TeV, *Eur. Phys. J. C* **78**, 466 (2018).
- [30] B. B. Abelev *et al.* (ALICE Collaboration), Production of inclusive $\Upsilon(1S)$ and $\Upsilon(2S)$ in p -Pb collisions at $\sqrt{s_{NN}} = 5.02$ TeV, *Phys. Lett. B* **740**, 105 (2015).
- [31] M. Aaboud *et al.* (ATLAS Collaboration), Measurement of quarkonium production in proton-lead and proton-proton collisions at 5.02 TeV with the ATLAS detector, *Eur. Phys. J. C* **78**, 171 (2018).
- [32] A. Tumasyan *et al.* (CMS Collaboration), Nuclear modification of Υ states in p -Pb collisions at $\sqrt{s_{NN}} = 5.02$ TeV, *Phys. Lett. B* **835**, 137397 (2022).
- [33] A. M. Sirunyan *et al.* (CMS Collaboration), Measurement of prompt and nonprompt J/ψ production in pp and p -Pb collisions at $\sqrt{s_{NN}} = 5.02$ TeV, *Eur. Phys. J. C* **77**, 269 (2017).
- [34] V. Khachatryan *et al.* (CMS Collaboration), Study of B Meson Production in $p + Pb$ Collisions at $\sqrt{s_{NN}} = 5.02$ TeV Using Exclusive Hadronic Decays, *Phys. Rev. Lett.* **116**, 032301 (2016).
- [35] A. M. Sirunyan *et al.* (CMS Collaboration), Measurements of the charm jet cross section and nuclear modification factor in p -Pb collisions at $\sqrt{s_{NN}} = 5.02$ TeV, *Phys. Lett. B* **772**, 306 (2017).
- [36] V. Khachatryan *et al.* (CMS Collaboration), Transverse momentum spectra of inclusive b jets in p -Pb collisions at $\sqrt{s_{NN}} = 5.02$ TeV, *Phys. Lett. B* **754**, 59 (2016).
- [37] J. Adams *et al.* (STAR Collaboration), Open Charm Yields in $d + Au$ Collisions at $\sqrt{s_{NN}} = 200$ GeV, *Phys. Rev. Lett.* **94**, 062301 (2005).
- [38] A. Adare *et al.* (PHENIX Collaboration), Cold-Nuclear-Matter Effects on Heavy-Quark Production in $d + Au$ Collisions at $\sqrt{s_{NN}} = 200$ GeV, *Phys. Rev. Lett.* **109**, 242301 (2012).
- [39] K. J. Eskola, I. Helenius, P. Paakkinen, and H. Paukkunen, A QCD analysis of LHCb D -meson data in $p + Pb$ collisions, *J. High Energy Phys.* **05** (2020) 037.
- [40] R. A. Khalek, R. Gauld, T. Giani, E. R. Nocera, T. R. Rabemananjara, and J. Rojo, nNNPDF3.0: Evidence for a modified partonic structure in heavy nuclei, *Eur. Phys. J. C* **82**, 507 (2022).
- [41] A. A. Alves, Jr. *et al.* (LHCb Collaboration), The LHCb detector at the LHC, *J. Instrum.* **3**, S08005 (2008).
- [42] R. Aaij *et al.* (LHCb Collaboration), LHCb detector performance, *Int. J. Mod. Phys. A* **30**, 1530022 (2015).
- [43] R. Aaij *et al.* (LHCb Collaboration), Precision luminosity measurements at LHCb, *J. Instrum.* **9**, P12005 (2014).
- [44] T. Sjöstrand, S. Mrenna, and P. Skands, PYTHIA physics and manual, *J. High Energy Phys.* **05** (2006) 026; T. Sjöstrand, S. Mrenna, and P. Skands, A brief introduction to PYTHIA 8.1, *Comput. Phys. Commun.* **178**, 852 (2008).
- [45] I. Belyaev *et al.*, Handling of the generation of primary events in Gauss, the LHCb simulation framework, *J. Phys. Conf. Ser.* **331**, 032047 (2011).

- [46] T. Pierog, Iu. Karpenko, J. M. Katzy, E. Yatsenko, and K. Werner *et al.*, EPOS LHC: Test of collective hadronization with data measured at the CERN Large Hadron Collider, *Phys. Rev. C* **92**, 034906 (2015).
- [47] D. J. Lange, The EvtGen particle decay simulation package, *Nucl. Instrum. Methods Phys. Res., Sect. A* **462**, 152 (2001).
- [48] P. Golonka and Z. Was, PHOTOS Monte Carlo: A precision tool for QED corrections in Z and W decays, *Eur. Phys. J. C* **45**, 97 (2006).
- [49] J. Allison *et al.* (GEANT4 Collaboration), GEANT4 developments and applications, *IEEE Trans. Nucl. Sci.* **53**, 270 (2006); S. Agostinelli *et al.* (GEANT4 Collaboration), GEANT4: A simulation toolkit, *Nucl. Instrum. Methods Phys. Res., Sect. A* **506**, 250 (2003).
- [50] M. Clemencic, G. Corti, S. Easo, C. R. Jones, S. Miglioranza, M. Pappagallo, and P. Robbe, The LHCb simulation application, Gauss: Design, evolution and experience, *J. Phys. Conf. Ser.* **331**, 032023 (2011).
- [51] R. L. Workman *et al.* (Particle Data Group), Review of particle physics, *Prog. Theor. Exp. Phys.* **2022**, 083C01 (2022).
- [52] T. Skwarnicki, A study of the radiative cascade transitions between the upsilon-prime and upsilon resonances, Ph.D. thesis, Institute of Nuclear Physics, Krakow, 1986 [Report No. DESY-F31-86-02].
- [53] M. Pivk and F. R. Le Diberder, sPlot: A statistical tool to unfold data distributions, *Nucl. Instrum. Methods Phys. Res., Sect. A* **555**, 356 (2005).
- [54] A. D. Bukin, Fitting function for asymmetric peaks, arXiv:0711.4449.
- [55] See Supplemental Material at <http://link.aps.org/supplemental/10.1103/PhysRevLett.131.102301> for a summary of systematic uncertainties and numerical results and additional plots for the fit result, nuclear modification factor, and forward-backward production ratio.
- [56] R. Aaij *et al.* (LHCb Collaboration), Measurement of the track reconstruction efficiency at LHCb, *J. Instrum.* **10**, P02007 (2015).
- [57] L. Anderlini *et al.*, The PIDCalib package, Report No. LHCb-PUB-2016-021, 2016.
- [58] R. Aaij *et al.*, Selection and processing of calibration samples to measure the particle identification performance of the LHCb experiment in Run 2, *Eur. Phys. J. Tech. Instrum.* **6**, 1 (2019).
- [59] R. Aaij *et al.* (LHCb Collaboration), Measurements of prompt charm production cross-sections in pp collisions at $\sqrt{s} = 5$ TeV, *J. High Energy Phys.* **06** (2017) 147.
- [60] R. Aaij *et al.* (LHCb Collaboration), Measurements of prompt charm production cross-sections in pp collisions at $\sqrt{s} = 13$ TeV, *J. High Energy Phys.* **03** (2016) 159; **09** (2016) 13; **05** (2017) 74.
- [61] K. J. Eskola, P. Paakkinen, H. Paukkunen, and C. A. Salgado, EPPS16: Nuclear parton distributions with LHC data, *Eur. Phys. J. C* **77**, 163 (2017).
- [62] K. Kovarik *et al.*, nCTEQ15—Global analysis of nuclear parton distributions with uncertainties in the CTEQ framework, *Phys. Rev. D* **93**, 085037 (2016).
- [63] B. Ducloué, T. Lappi, and H. Mäntysaari, Forward J/ψ and D meson nuclear suppression at the LHC, *Nucl. Part. Phys. Proc.* **289–290**, 309 (2017).
- [64] Y.-Q. Ma, P. Tribedy, R. Venugopalan, and K. Watanabe, Event engineering studies for heavy flavor production and hadronization in high multiplicity hadron-hadron and hadron-nucleus collisions, *Phys. Rev. D* **98**, 074025 (2018).
- [65] H.-S. Shao, HELAC-Onia: An automatic matrix element generator for heavy quarkonium physics, *Comput. Phys. Commun.* **184**, 2562 (2013).
- [66] H.-S. Shao, HELAC-Onia 2.0: An upgraded matrix-element and event generator for heavy quarkonium physics, *Comput. Phys. Commun.* **198**, 238 (2016).
- [67] J.-P. Lansberg and H.-S. Shao, Towards an automated tool to evaluate the impact of the nuclear modification of the gluon density on quarkonium, D and B meson production in proton-nucleus collisions, *Eur. Phys. J. C* **77**, 1 (2017).
- [68] A. Kusina, J.-P. Lansberg, I. Schienbein, and H.-S. Shao, Gluon Shadowing in Heavy-Flavor Production at the LHC, *Phys. Rev. Lett.* **121**, 052004 (2018).
- [69] B. Ducloué, T. Lappi, and H. Mäntysaari, Forward J/ψ production in proton-nucleus collisions at high energy, *Phys. Rev. D* **91**, 114005 (2015).
- [70] H. Kowalski, T. Lappi, and R. Venugopalan, Nuclear Enhancement of Universal Dynamics of High Parton Densities, *Phys. Rev. Lett.* **100**, 022303 (2008).

R. Aaij³², A. S. W. Abdelmotteleb⁵⁰, C. Abellan Beteta⁴⁴, F. Abudinén⁵⁰, T. Ackernley⁵⁴, B. Adeva⁴⁰, M. Adinolfi⁴⁸, H. Afsharnia⁹, C. Agapopoulou¹³, C. A. Aidala⁷⁶, S. Aiola²⁵, Z. Ajaltouni⁹, S. Akar⁵⁹, K. Akiba³², J. Albrecht¹⁵, F. Alessio⁴², M. Alexander⁵³, A. Alfonso Albergo³⁹, Z. Aliouche⁵⁶, P. Alvarez Cartelle⁴⁹, S. Amato², J. L. Amey⁴⁸, Y. Amhis^{11,42}, L. An⁴², L. Anderlini²², M. Andersson⁴⁴, A. Andreianov³⁸, M. Andreotti²¹, D. Andreou⁶², D. Ao⁶, F. Archilli¹⁷, A. Artamonov³⁸, M. Artuso⁶², E. Aslanides¹⁰, M. Atzeni⁴⁴, B. Audurier¹², S. Bachmann¹⁷, M. Bachmayer⁴³, J. J. Back⁵⁰, A. Bailly-reyre¹³, P. Baladron Rodriguez⁴⁰, V. Balagura¹², W. Baldini²¹, J. Baptista de Souza Leite¹, M. Barbetti^{22,b}, R. J. Barlow⁵⁶, S. Barsuk¹¹, W. Barter⁵⁵, M. Bartolini⁴⁹, F. Baryshnikov³⁸, J. M. Basels¹⁴, G. Bassi^{29,c}, B. Batsukh⁴, A. Battig¹⁵, A. Bay⁴³, A. Beck⁵⁰, M. Becker¹⁵, F. Bedeschi²⁹, I. B. Bediaga¹, A. Beiter⁶², V. Belavin³⁸, S. Belin⁴⁰, V. Bellee⁴⁴, K. Belous³⁸, I. Belov³⁸, I. Belyaev³⁸, G. Bencivenni²³, E. Ben-Haim¹³, A. Berezhnoy³⁸, R. Bernet⁴⁴, D. Berninghoff¹⁷, H. C. Bernstein⁶², C. Bertella⁵⁶, A. Bertolin²⁸, C. Betancourt⁴⁴

F. Betti⁴², I. Bezshyiko⁴⁴, S. Bhasin⁴⁸, J. Bhom³⁵, L. Bian⁶⁷, M. S. Bieker¹⁵, N. V. Biesuz²¹, S. Bifani⁴⁷, P. Billoir¹³, A. Biolchini³², M. Birch⁵⁵, F. C. R. Bishop⁴⁹, A. Bitadze⁵⁶, A. Bizzeti⁵⁶, M. P. Blago⁴⁹, T. Blake⁵⁰, F. Blanc⁴³, S. Blusk⁶², D. Bobulska⁵³, J. A. Boelhaue¹⁵, O. Boente Garcia⁴⁰, T. Boettcher⁵⁹, A. Boldyrev³⁸, N. Bondar^{38,42}, S. Borghi⁵⁶, M. Borsato¹⁷, J. T. Borsuk³⁵, S. A. Bouchiba⁴³, T. J. V. Bowcock^{54,42}, A. Boyer⁴², C. Bozzi²¹, M. J. Bradley⁵⁵, S. Braun⁶⁰, A. Brea Rodriguez⁴⁰, J. Brodzicka³⁵, A. Brossa Gonzalo⁵⁰, D. Brundu²⁷, A. Buonaura⁴⁴, L. Buonincontri²⁸, A. T. Burke⁵⁶, C. Burr⁴², A. Bursche⁶⁶, A. Butkevich³⁸, J. S. Butter³², J. Buytaert⁴², W. Byczynski⁴², S. Cadeddu²⁷, H. Cai⁶⁷, R. Calabrese^{21,d}, L. Calefice^{15,13}, S. Cali²³, R. Calladine⁴⁷, M. Calvi^{26,e}, M. Calvo Gomez⁷⁴, P. Camargo Magalhaes⁴⁸, P. Campana²³, D. H. Campora Perez⁷³, A. F. Campoverde Quezada⁶, S. Capelli^{26,e}, L. Capriotti^{20,f}, A. Carbone^{20,f}, G. Carboni³¹, R. Cardinale^{24,g}, A. Cardini²⁷, I. Carli⁴, P. Carniti^{26,e}, L. Carus¹⁴, A. Casais Vidal⁴⁰, R. Caspary¹⁷, G. Casse¹⁷, M. Cattaneo⁴², G. Cavallero⁴², V. Cavallini^{21,d}, S. Celani⁴³, J. Cerasoli¹⁰, D. Cervenkov⁵⁷, A. J. Chadwick⁵⁴, M. G. Chapman⁴⁸, M. Charles¹³, Ph. Charpentier⁴², C. A. Chavez Barajas⁵⁴, M. Chefdeville⁸, C. Chen³, S. Chen⁴, A. Chernov³⁵, S. Chernyshenko⁴⁶, V. Chobanova⁴⁰, S. Cholak⁴³, M. Chrzaszcz³⁵, A. Chubykin³⁸, V. Chulikov³⁸, P. Ciambrone²³, M. F. Cicala⁵⁰, X. Cid Vidal⁴⁰, G. Ciezarek⁴², G. Ciullo^{21,d}, P. E. L. Clarke⁵², M. Clemencic⁴², H. V. Cliff⁴⁹, J. Closier⁴², J. L. Cobbedick⁵⁶, V. Coco⁴², J. A. B. Coelho¹¹, J. Cogan¹⁰, E. Cogneras⁹, L. Cojocariu³⁷, P. Collins⁴², T. Colombo⁴², L. Congedo¹⁹, A. Contu²⁷, N. Cooke⁴⁷, G. Coombs⁵³, I. Corredoira⁴⁰, G. Corti⁴², B. Couturier⁴², D. C. Craik⁵⁸, J. Crkovská⁶¹, M. Cruz Torres^{1,h}, R. Currie⁵², C. L. Da Silva⁶¹, S. Dadabaev³⁸, L. Dai⁶⁵, E. Dall'Occo¹⁵, J. Dalseno⁴⁰, C. D'Ambrosio⁴², A. Danilina³⁸, P. d'Argent¹⁵, J. E. Davies⁵⁶, A. Davis⁵⁶, O. De Aguiar Francisco⁵⁶, J. de Boer⁴², K. De Bruyn⁷², S. De Capua⁵⁶, M. De Cian⁴³, U. De Freitas Carneiro Da Graca¹, E. De Lucia²³, J. M. De Miranda¹, L. De Paula², M. De Serio^{19,i}, D. De Simone⁴⁴, P. De Simone²³, F. De Vellis¹⁵, J. A. de Vries⁷³, C. T. Dean⁶¹, F. Debernardis^{19,i}, D. Decamp⁸, V. Dedu¹⁰, L. Del Buono¹³, B. Delaney⁵⁸, H.-P. Dembinski¹⁵, V. Denysenko⁴⁴, O. Deschamps⁹, F. Dettori^{27,j}, B. Dey⁷⁰, A. Di Cicco²³, P. Di Nezza²³, S. Didenko³⁸, L. Dieste Maronas⁴⁰, S. Ding⁶², V. Dobishuk⁴⁶, A. Dolmatov³⁸, C. Dong³, A. M. Donohoe¹⁸, F. Dordei²⁷, A. C. dos Reis¹, L. Douglas⁵³, A. G. Downes⁸, M. W. Dudek³⁵, L. Dufour⁴², V. Duk⁷¹, P. Durante⁴², J. M. Durham⁶¹, D. Dutta⁵⁶, A. Dziurda³⁵, A. Dzyuba³⁸, S. Easo⁵¹, U. Egede⁶³, V. Egorychev³⁸, S. Eidelman^{38,a}, S. Eisenhardt⁵², S. Ek-In⁴³, L. Eklund⁷⁵, S. Ely⁶², A. Ene³⁷, E. Epple⁶¹, S. Escher¹⁴, J. Eschle⁴⁴, S. Esen⁴⁴, T. Evans⁵⁶, L. N. Falcao¹, Y. Fan⁶, B. Fang⁶⁷, S. Farry⁵⁴, D. Fazzini^{26,e}, M. Feo⁴², A. D. Fernez⁶⁰, F. Ferrari²⁰, L. Ferreira Lopes⁴³, F. Ferreira Rodrigues², S. Ferreres Sole³², M. Ferrillo⁴⁴, M. Ferro-Luzzi⁴², S. Filippov³⁸, R. A. Fini¹⁹, M. Fiorini^{21,d}, M. Firlej³⁴, K. M. Fischer⁵⁷, D. S. Fitzgerald⁷⁶, C. Fitzpatrick⁵⁶, T. Fiutowski³⁴, F. Fleuret¹², M. Fontana¹³, F. Fontanelli^{24,g}, R. Forty⁴², D. Foulds-Holt⁴⁹, V. Franco Lima⁵⁴, M. Franco Sevilla⁶⁰, M. Frank⁴², E. Franzoso^{21,d}, G. Frau¹⁷, C. Frei⁴², D. A. Friday⁵³, J. Fu⁶, Q. Fuehring¹⁵, E. Gabriel³², G. Galati^{19,i}, A. Gallas Torreira⁴⁰, D. Galli^{20,f}, S. Gambetta^{52,42}, Y. Gan³, M. Gandelman², P. Gandini²⁵, Y. Gao⁵, M. Garau^{27,j}, L. M. Garcia Martin⁵⁰, P. Garcia Moreno³⁹, J. García Pardiñas^{26,e}, B. Garcia Plana⁴⁰, F. A. Garcia Rosales¹², L. Garrido³⁹, C. Gaspar⁴², R. E. Geertsema³², D. Gerick¹⁷, L. L. Gerken¹⁵, E. Gersabeck⁵⁶, M. Gersabeck⁵⁶, T. Gershon⁵⁰, L. Giambastiani²⁸, V. Gibson⁴⁹, H. K. Gienza³⁶, A. L. Gilman⁵⁷, M. Giovannetti^{23,k}, A. Gioventù⁴⁰, P. Gironella Gironell³⁹, C. Giugliano^{21,d}, M. A. Giza³⁵, K. Gizdov⁵², E. L. Gkougkousis⁴², V. V. Gligorov^{13,42}, C. Göbel⁶⁴, E. Golobardes⁷⁴, D. Golubkov³⁸, A. Golutvin^{55,38}, A. Gomes^{1,l}, S. Gomez Fernandez³⁹, F. Goncalves Abrantes⁵⁷, M. Goncerz³⁵, G. Gong³, I. V. Gorelov³⁸, C. Gotti²⁶, J. P. Grabowski¹⁷, T. Grammatico¹³, L. A. Granado Cardoso⁴², E. Graugés³⁹, E. Graverini⁴³, G. Graziani⁴³, A. T. Grecu³⁷, L. M. Greeven³², N. A. Grieser⁴, L. Grillo⁵³, S. Gromov³⁸, B. R. Gruberg Cazon⁵⁷, C. Gu³, M. Guarise^{21,d}, M. Guittiere¹¹, P. A. Günther¹⁷, E. Gushchin³⁸, A. Guth¹⁴, Y. Guz³⁸, T. Gys⁴², T. Hadavizadeh⁶³, G. Haefeli⁴³, C. Haen⁴², J. Haimberger⁴², S. C. Haines⁴⁹, T. Halewood-leagas⁵⁴, M. M. Halvorsen⁴², P. M. Hamilton⁶⁰, J. Hammerich⁵⁴, Q. Han⁷, X. Han¹⁷, E. B. Hansen⁵⁶, S. Hansmann-Menzemer^{17,42}, L. Hao⁶, N. Harnew⁵⁷, T. Harrison⁵⁴, C. Hasse⁴², M. Hatch⁴², J. He^{6,m}, K. Heijhoff³², K. Heinicke¹⁵, R. D. L. Henderson^{63,50}, A. M. Hennequin⁵⁸, K. Hennessy⁵⁴, L. Henry⁴², J. Heuel¹⁴, A. Hicheur², D. Hill⁴³, M. Hilton⁵⁶, S. E. Hollitt¹⁵, R. Hou⁷, Y. Hou⁸, J. Hu¹⁷, J. Hu⁶⁶, W. Hu⁵, X. Hu³, W. Huang⁶⁷, X. Huang⁶⁷, W. Hulsbergen³², R. J. Hunter⁵⁰, M. Hushchyn³⁸, D. Hutchcroft⁵⁴, P. Ibis¹⁵, M. Idzik³⁴, D. Ilin³⁸, P. Ilten⁵⁹, A. Inglese³⁸, A. Iniukhin³⁸, A. Ishteev³⁸, K. Ivshin³⁸, R. Jacobsson⁴², H. Jage¹⁴, S. J. Jaimes Elles⁴¹, S. Jakobsen⁴², E. Jans³²

B. K. Jashal⁴¹, A. Jawahery⁶⁰, V. Jevtic¹⁵, X. Jiang^{4,6}, M. John⁵⁷, D. Johnson⁵⁸, C. R. Jones⁴⁹, T. P. Jones⁵⁰,
 B. Jost⁴², N. Jurik⁴², I. Juszczak³⁵, S. Kandybei⁴⁵, Y. Kang³, M. Karacson⁴², D. Karpenkov³⁸, M. Karpov³⁸,
 J. W. Kautz⁵⁹, F. Keizer⁴², D. M. Keller⁶², M. Kenzie⁵⁰, T. Ketel³³, B. Khanji¹⁵, A. Kharisova³⁸,
 S. Kholodenko³⁸, T. Kim¹⁴, V. S. Kirsebom⁴³, O. Kitouni⁵⁸, S. Klaver³³, N. Kleijne^{29,c}, K. Klimaszewski³⁶,
 M. R. Kmiec³⁶, S. Koliiev⁴⁶, A. Kondybayeva³⁸, A. Konoplyannikov³⁸, P. Kopciwicz³⁴, R. Kopečna¹⁷,
 P. Koppenburg³², M. Korolev³⁸, I. Kostiuk^{32,46}, O. Kot⁴⁶, S. Kotriakhova⁴⁶, A. Kozachuk³⁸, P. Kravchenko³⁸,
 L. Kravchuk³⁸, R. D. Krawczyk⁴², M. Kreps⁵⁰, S. Kretschmar¹⁴, P. Krokovny³⁸, W. Krupa³⁴, W. Krzemien³⁶,
 J. Kubat¹⁷, W. Kucewicz^{35,34}, M. Kucharczyk³⁵, V. Kudryavtsev³⁸, G. J. Kunde⁶¹, D. Lacarrere⁴², G. Lafferty⁵⁶,
 A. Lai²⁷, A. Lampis^{27,j}, D. Lancierini⁴⁴, J. J. Lane⁵⁶, R. Lane⁴⁸, G. Lanfranchi²³, C. Langenbruch¹⁴,
 J. Langer¹⁵, O. Lantwin³⁸, T. Latham⁵⁰, F. Lazzari^{29,n}, M. Lazzaroni^{25,o}, R. Le Gac¹⁰, S. H. Lee⁷⁶, R. Lefèvre⁹,
 A. Leflat³⁸, S. Legotin³⁸, P. Lenisa^{21,d}, O. Leroy¹⁰, T. Lesiak³⁵, B. Leverington¹⁷, H. Li⁶⁶, K. Li⁷, P. Li¹⁷,
 S. Li⁷, Y. Li⁴, Z. Li⁶², X. Liang⁶², C. Lin⁶, T. Lin⁵¹, R. Lindner⁴², V. Lisovskyi¹⁵, R. Litvinov^{27,j}, G. Liu⁶⁶,
 H. Liu⁶, Q. Liu⁶, S. Liu^{4,6}, A. Lobo Salvia³⁹, A. Loi²⁷, R. Lollini⁷¹, J. Lomba Castro⁴⁰, I. Longstaff⁵³,
 J. H. Lopes², S. López Soliño⁴⁰, G. H. Lovell⁴⁹, Y. Lu^{4,p}, C. Lucarelli^{22,b}, D. Lucchesi^{28,q}, S. Luchuk³⁸,
 M. Lucio Martinez³², V. Lukashenko^{32,46}, Y. Luo³, A. Lupato⁵⁶, E. Luppi^{21,d}, A. Lusiani^{29,c}, K. Lynch¹⁸,
 X.-R. Lyu⁶, L. Ma⁴, R. Ma⁶, S. Maccolini²⁰, F. Machefert¹¹, F. Maciuc³⁷, V. Macko⁴³, P. Mackowiak¹⁵,
 S. Maddrell-Mander⁴⁸, L. R. Madhan Mohan⁴⁸, A. Maevskiy³⁸, D. Maisuzenko³⁸, M. W. Majewski³⁴,
 J. J. Malczewski³⁵, S. Malde⁵⁷, B. Malecki³⁵, A. Malinin³⁸, T. Maltsev³⁸, H. Malygina¹⁷, G. Manca^{27,j},
 G. Mancinelli¹⁰, D. Manuzzi²⁰, C. A. Manzari⁴⁴, D. Marangotto^{25,o}, J. F. Marchand⁸, U. Marconi²⁰,
 S. Mariani^{22,b}, C. Marin Benito³⁹, M. Marinangeli⁴³, J. Marks¹⁷, A. M. Marshall⁴⁸, P. J. Marshall⁵⁴,
 G. Martelli^{71,r}, G. Martellotti³⁰, L. Martinazzoli^{42,e}, M. Martinelli^{26,e}, D. Martinez Santos⁴⁰, F. Martinez Vidal⁴¹,
 A. Massafferri¹, M. Materok¹⁴, R. Matev⁴², A. Mathad⁴⁴, V. Matiunin³⁸, C. Matteuzzi²⁶, K. R. Mattioli⁷⁶,
 A. Mauri³², E. Maurice¹², J. Mauricio³⁹, M. Mazurek⁴², M. McCann⁵⁵, L. McConnell¹⁸, T. H. McGrath⁵⁶,
 N. T. McHugh⁵³, A. McNab⁵⁶, R. McNulty¹⁸, J. V. Mead⁵⁴, B. Meadows⁵⁹, G. Meier¹⁵, D. Melnychuk³⁶,
 S. Meloni^{26,e}, M. Merk^{32,73}, A. Merli^{25,o}, L. Meyer Garcia², M. Mikhasenko^{69,s}, D. A. Milanes⁶⁸, E. Millard⁵⁰,
 M. Milovanovic⁴², M.-N. Minard^{8,a}, A. Minotti^{26,e}, S. E. Mitchell⁵², B. Mitreska⁵⁶, D. S. Mitzel¹⁵, A. Mödden¹⁵,
 R. A. Mohammed⁵⁷, R. D. Moise⁵⁵, S. Mokhnenko³⁸, T. Mombächer⁴⁰, I. A. Monroy⁶⁸, S. Monteil⁹,
 M. Morandin²⁸, G. Morello²³, M. J. Morello^{29,c}, J. Moron³⁴, A. B. Morris⁶⁹, A. G. Morris⁵⁰, R. Mountain⁶²,
 H. Mu³, F. Muheim⁵², M. Mulder⁷², K. Müller⁴⁴, C. H. Murphy⁵⁷, D. Murray⁵⁶, R. Murta⁵⁵, P. Muzzetto^{27,j},
 P. Naik⁴⁸, T. Nakada⁴³, R. Nandakumar⁵¹, T. Nanut⁴², I. Nasteva², M. Needham⁵², N. Neri^{25,o}, S. Neubert⁶⁹,
 N. Neufeld⁴², P. Neustroev³⁸, R. Newcombe⁵⁵, E. M. Niel⁴³, S. Nieswand¹⁴, N. Nikitin³⁸, N. S. Nolte⁵⁸,
 C. Normand^{8,27,j}, C. Nunez⁷⁶, A. Oblakowska-Mucha³⁴, V. Obraztsov³⁸, T. Oeser¹⁴, D. P. O'Hanlon⁴⁸,
 S. Okamura^{21,d}, R. Oldeman^{27,j}, F. Oliva⁵², M. E. Olivares⁶², C. J. G. Onderwater⁷², R. H. O'Neil⁵²,
 J. M. Otalora Goicochea², T. Ovsianikova³⁸, P. Owen⁴⁴, A. Oyanguren⁴¹, O. Ozcelik⁵², K. O. Padeken⁶⁹,
 B. Pagare⁵⁰, P. R. Pais⁴², T. Pajero⁵⁷, A. Palano¹⁹, M. Palutan²³, Y. Pan⁵⁶, G. Panshin³⁸, A. Papanestis⁵¹,
 M. Pappagallo^{19,i}, L. L. Pappalardo^{21,d}, C. Pappenheimer⁵⁹, W. Parker⁶⁰, C. Parkes⁵⁶, B. Passalacqua^{21,d},
 G. Passaleva²², A. Pastore¹⁹, M. Patel⁵⁵, C. Patrignani^{20,f}, C. J. Pawley⁷³, A. Pearce⁴², A. Pellegrino³²,
 M. Pepe Altarelli⁴², S. Perazzini²⁰, D. Pereima³⁸, A. Pereiro Castro⁴⁰, P. Perret⁹, M. Petric⁵³, K. Petridis⁴⁸,
 A. Petrolini^{24,g}, A. Petrov³⁸, S. Petrucci⁵², M. Petruzzo²⁵, H. Pham⁶², A. Philippov³⁸, R. Piandani⁶, L. Pica^{29,c},
 M. Piccini⁷¹, B. Pietrzyk⁸, G. Pietrzyk¹¹, M. Pili⁵⁷, D. Pinci³⁰, F. Pisani⁴², M. Pizzichemi^{26,42,e}, V. Placinta³⁷,
 J. Plews⁴⁷, M. Plo Casasus⁴⁰, F. Polci^{13,42}, M. Poli Lener²³, M. Poliakov⁶², A. Poluektov¹⁰, N. Polukhina³⁸,
 I. Polyakov⁶², E. Polycarpo², S. Ponce⁴², D. Popov^{6,42}, S. Popov³⁸, S. Poslavskii³⁸, K. Prasanth³⁵,
 L. Promberger⁴², C. Prouve⁴⁰, V. Pugatch⁴⁶, V. Puill¹¹, G. Punzi^{29,t}, H. R. Qi³, W. Qian⁶, N. Qin³, S. Qu³,
 R. Quagliani⁴³, N. V. Raab¹⁸, R. I. Rabadan Trejo⁶, B. Rachwal³⁴, J. H. Rademacker⁴⁸, R. Rajagopalan⁶²,
 M. Rama²⁹, M. Ramos Pernas⁵⁰, M. S. Rangel², F. Ratnikov³⁸, G. Raven^{33,42}, M. Rebollo De Miguel⁴¹,
 F. Redi⁴², F. Reiss⁵⁶, C. Remon Alepuz⁴¹, Z. Ren³, V. Renaudin⁵⁷, P. K. Resmi¹⁰, R. Ribatti^{29,c}, A. M. Ricci²⁷,
 S. Ricciardi⁵¹, K. Rinnert⁵⁴, P. Robbe¹¹, G. Robertson⁵², A. B. Rodrigues⁴³, E. Rodrigues⁵⁴,
 J. A. Rodriguez Lopez⁶⁸, E. Rodriguez Rodriguez⁴⁰, A. Rollings⁵⁷, P. Roloff⁴², V. Romanovskiy³⁸,
 M. Romero Lamas⁴⁰, A. Romero Vidal⁴⁰, J. D. Roth^{76,a}, M. Rotondo²³, M. S. Rudolph⁶², T. Ruf⁴²

R. A. Ruiz Fernandez⁴⁰, J. Ruiz Vidal,⁴¹ A. Ryzhikov³⁸, J. Ryzka³⁴, J. J. Saborido Silva⁴⁰, N. Sagidova³⁸,
 N. Sahoo⁴⁷, B. Saitta^{27,j}, M. Salomoni⁴², C. Sanchez Gras³², I. Sanderswood⁴¹, R. Santacesaria³⁰,
 C. Santamarina Rios⁴⁰, M. Santimaria²³, E. Santovetti^{31,k}, D. Saranin³⁸, G. Sarpis¹⁴, M. Sarpis⁶⁹, A. Sarti³⁰,
 C. Satriano^{30,u}, A. Satta³¹, M. Saur¹⁵, D. Savrina³⁸, H. Sazak⁹, L. G. Scantlebury Smead⁵⁷, A. Scarabotto¹³,
 S. Schael¹⁴, S. Scherl⁵⁴, M. Schiller⁵³, H. Schindler⁴², M. Schmelling¹⁶, B. Schmidt⁴², S. Schmitt¹⁴,
 O. Schneider⁴³, A. Schopper⁴², M. Schubiger³², S. Schulte⁴³, M. H. Schune¹¹, R. Schwemmer⁴²,
 B. Sciascia^{23,42}, A. Sciuccati⁴², S. Sellam⁴⁰, A. Semennikov³⁸, M. Senghi Soares³³, A. Sergi^{24,g}, N. Serra⁴⁴,
 L. Sestini²⁸, A. Seuthe¹⁵, Y. Shang⁵, D. M. Shangase⁷⁶, M. Shapkin³⁸, I. Shchemerov³⁸, L. Shchutka⁴³,
 T. Shears⁵⁴, L. Shekhtman³⁸, Z. Shen⁵, S. Sheng^{4,6}, V. Shevchenko³⁸, E. B. Shields^{26,e}, Y. Shimizu¹¹,
 E. Shmanin³⁸, J. D. Shupperd⁶², B. G. Siddi^{21,d}, R. Silva Coutinho⁴⁴, G. Simi²⁸, S. Simone^{19,i}, M. Singla⁶³,
 N. Skidmore⁵⁶, R. Skuza¹⁷, T. Skwarnicki⁶², M. W. Slater⁴⁷, I. Slazyk^{21,d}, J. C. Smallwood⁵⁷, J. G. Smeaton⁴⁹,
 E. Smith⁴⁴, M. Smith⁵⁵, A. Snoch³², L. Soares Lavra⁹, M. D. Sokoloff⁵⁹, F. J. P. Soler⁵³, A. Solomin^{38,48},
 A. Solovov³⁸, I. Solovyev³⁸, F. L. Souza De Almeida², B. Souza De Paula², B. Spaan^{15,a}, E. Spadaro Norella^{25,o},
 E. Spiridenkov³⁸, P. Spradlin⁵³, V. Sriskaran⁴², F. Stagni⁴², M. Stahl⁵⁹, S. Stahl⁴², S. Stanislaus⁵⁷,
 O. Steinkamp⁴⁴, O. Stenyakin³⁸, H. Stevens¹⁵, S. Stone^{62,a}, D. Strelakina³⁸, F. Suljik⁵⁷, J. Sun²⁷, L. Sun⁶⁷,
 Y. Sun⁶⁰, P. Sviha⁵⁶, P. N. Swallow⁴⁷, K. Swientek³⁴, A. Szabelski³⁶, T. Szumlak³⁴, M. Szymanski⁴²,
 S. Taneja⁵⁶, A. R. Tanner⁴⁸, M. D. Tat⁵⁷, A. Terentev³⁸, F. Teubert⁴², E. Thomas⁴², D. J. D. Thompson⁴⁷,
 K. A. Thomson⁵⁴, H. Tilquin⁵⁵, V. Tisserand⁹, S. T'Jampens⁸, M. Tobin⁴, L. Tomassetti^{21,d}, G. Tonani^{25,o},
 X. Tong⁵, D. Torres Machado¹, D. Y. Tou³, E. Trifonova³⁸, S. M. Trilov⁴⁸, C. Trippel⁴³, G. Tuci⁶, A. Tully⁴³,
 N. Tuning^{32,42}, A. Ukleja³⁶, D. J. Unverzagt¹⁷, E. Ursov³⁸, A. Usachov³², A. Ustyuzhanin³⁸, U. Uwer¹⁷,
 A. Vagner³⁸, V. Vagnoni²⁰, A. Valassi⁴², G. Valenti²⁰, N. Valls Canudas⁷⁴, M. van Beuzekom³², M. Van Dijk⁴³,
 H. Van Hecke⁶¹, E. van Herwijnen³⁸, M. van Veghel⁷², R. Vazquez Gomez³⁹, P. Vazquez Regueiro⁴⁰,
 C. Vázquez Sierra⁴², S. Vecchi²¹, J. J. Velthuis⁴⁸, M. Veltri^{22,v}, A. Venkateswaran⁶², M. Veronesi³²,
 M. Vesterinen⁵⁰, D. Vieira⁵⁹, M. Vieites Diaz⁴³, X. Vilasis-Cardona⁷⁴, E. Vilella Figueras⁵⁴, A. Villa²⁰,
 P. Vincent¹³, F. C. Volle¹¹, D. vom Bruch¹⁰, A. Vorobyev³⁸, V. Vorobyev³⁸, N. Voropaev³⁸, K. Vos⁷³, R. Waldi¹⁷,
 J. Walsh²⁹, C. Wang¹⁷, J. Wang⁵, J. Wang⁴, J. Wang³, J. Wang⁶⁷, M. Wang⁵, R. Wang⁴⁸, Y. Wang⁷, Z. Wang⁴⁴,
 Z. Wang³, Z. Wang⁶, J. A. Ward^{50,63}, N. K. Watson⁴⁷, D. Websdale⁵⁵, C. Weissner⁵⁸, B. D. C. Westhenry⁴⁸,
 D. J. White⁵⁶, M. Whitehead⁵³, A. R. Wiederhold⁵⁰, D. Wiedner¹⁵, G. Wilkinson⁵⁷, M. K. Wilkinson⁵⁹,
 I. Williams⁴⁹, M. Williams⁵⁸, M. R. J. Williams⁵², R. Williams⁴⁹, F. F. Wilson⁵¹, W. Wislicki³⁶, M. Witek³⁵,
 L. Witola¹⁷, C. P. Wong⁶¹, G. Wormser¹¹, S. A. Wotton⁴⁹, H. Wu⁶², K. Wyllie⁴², Z. Xiang⁶, D. Xiao⁷,
 Y. Xie⁷, A. Xu⁵, J. Xu⁶, L. Xu³, M. Xu⁵⁰, Q. Xu⁶, Z. Xu⁹, Z. Xu⁶, D. Yang³, S. Yang⁶, Y. Yang⁶, Z. Yang⁵,
 Z. Yang⁶⁰, L. E. Yeomans⁵⁴, H. Yin⁷, J. Yu⁶⁵, X. Yuan⁶², E. Zaffaroni⁴³, M. Zavertyaev¹⁶, M. Zdybal³⁵,
 O. Zenaiev⁴², M. Zeng³, D. Zhang⁷, L. Zhang³, S. Zhang⁶⁵, S. Zhang⁵, Y. Zhang⁵, Y. Zhang⁵⁷, A. Zharkova³⁸,
 A. Zhelezov¹⁷, Y. Zheng⁶, T. Zhou⁵, X. Zhou⁶, Y. Zhou⁶, V. Zhovkovska¹¹, X. Zhu³, X. Zhu⁷, Z. Zhu⁶,
 V. Zhukov^{14,38}, Q. Zou^{4,6}, S. Zucchelli^{20,f}, D. Zuliani²⁸, and G. Zunica⁵⁶

(LHCb Collaboration)

¹Centro Brasileiro de Pesquisas Físicas (CBPF), Rio de Janeiro, Brazil

²Universidade Federal do Rio de Janeiro (UFRJ), Rio de Janeiro, Brazil

³Center for High Energy Physics, Tsinghua University, Beijing, China

⁴Institute Of High Energy Physics (IHEP), Beijing, China

⁵School of Physics State Key Laboratory of Nuclear Physics and Technology, Peking University, Beijing, China

⁶University of Chinese Academy of Sciences, Beijing, China

⁷Institute of Particle Physics, Central China Normal University, Wuhan, Hubei, China

⁸Université Savoie Mont Blanc, CNRS, IN2P3-LAPP, Annecy, France

⁹Université Clermont Auvergne, CNRS/IN2P3, LPC, Clermont-Ferrand, France

¹⁰Aix Marseille Université, CNRS/IN2P3, CPPM, Marseille, France

¹¹Université Paris-Saclay, CNRS/IN2P3, IJCLab, Orsay, France

¹²Laboratoire Leprince-Ringuet, CNRS/IN2P3, Ecole Polytechnique, Institut Polytechnique de Paris, Palaiseau, France

¹³LPNHE, Sorbonne Université, Paris Diderot Sorbonne Paris Cité, CNRS/IN2P3, Paris, France

- ¹⁴*I. Physikalisches Institut, RWTH Aachen University, Aachen, Germany*
- ¹⁵*Fakultät Physik, Technische Universität Dortmund, Dortmund, Germany*
- ¹⁶*Max-Planck-Institut für Kernphysik (MPIK), Heidelberg, Germany*
- ¹⁷*Physikalisches Institut, Ruprecht-Karls-Universität Heidelberg, Heidelberg, Germany*
- ¹⁸*School of Physics, University College Dublin, Dublin, Ireland*
- ¹⁹*INFN Sezione di Bari, Bari, Italy*
- ²⁰*INFN Sezione di Bologna, Bologna, Italy*
- ²¹*INFN Sezione di Ferrara, Ferrara, Italy*
- ²²*INFN Sezione di Firenze, Firenze, Italy*
- ²³*INFN Laboratori Nazionali di Frascati, Frascati, Italy*
- ²⁴*INFN Sezione di Genova, Genova, Italy*
- ²⁵*INFN Sezione di Milano, Milano, Italy*
- ²⁶*INFN Sezione di Milano-Bicocca, Milano, Italy*
- ²⁷*INFN Sezione di Cagliari, Monserrato, Italy*
- ²⁸*Università degli Studi di Padova, Università e INFN, Padova, Padova, Italy*
- ²⁹*INFN Sezione di Pisa, Pisa, Italy*
- ³⁰*INFN Sezione di Roma La Sapienza, Roma, Italy*
- ³¹*INFN Sezione di Roma Tor Vergata, Roma, Italy*
- ³²*Nikhef National Institute for Subatomic Physics, Amsterdam, Netherlands*
- ³³*Nikhef National Institute for Subatomic Physics and VU University Amsterdam, Amsterdam, Netherlands*
- ³⁴*AGH–University of Science and Technology, Faculty of Physics and Applied Computer Science, Kraków, Poland*
- ³⁵*Henryk Niewodniczanski Institute of Nuclear Physics Polish Academy of Sciences, Kraków, Poland*
- ³⁶*National Center for Nuclear Research (NCBJ), Warsaw, Poland*
- ³⁷*Horia Hulubei National Institute of Physics and Nuclear Engineering, Bucharest-Magurele, Romania*
- ³⁸*Affiliated with an institute covered by a cooperation agreement with CERN*
- ³⁹*ICCUB, Universitat de Barcelona, Barcelona, Spain*
- ⁴⁰*Instituto Galego de Física de Altas Enerxías (IGFAE), Universidade de Santiago de Compostela, Santiago de Compostela, Spain*
- ⁴¹*Instituto de Física Corpuscular, Centro Mixto Universidad de Valencia—CSIC, Valencia, Spain*
- ⁴²*European Organization for Nuclear Research (CERN), Geneva, Switzerland*
- ⁴³*Institute of Physics, Ecole Polytechnique Fédérale de Lausanne (EPFL), Lausanne, Switzerland*
- ⁴⁴*Physik-Institut, Universität Zürich, Zürich, Switzerland*
- ⁴⁵*NSC Kharkiv Institute of Physics and Technology (NSC KIPT), Kharkiv, Ukraine*
- ⁴⁶*Institute for Nuclear Research of the National Academy of Sciences (KINR), Kyiv, Ukraine*
- ⁴⁷*University of Birmingham, Birmingham, United Kingdom*
- ⁴⁸*H.H. Wills Physics Laboratory, University of Bristol, Bristol, United Kingdom*
- ⁴⁹*Cavendish Laboratory, University of Cambridge, Cambridge, United Kingdom*
- ⁵⁰*Department of Physics, University of Warwick, Coventry, United Kingdom*
- ⁵¹*STFC Rutherford Appleton Laboratory, Didcot, United Kingdom*
- ⁵²*School of Physics and Astronomy, University of Edinburgh, Edinburgh, United Kingdom*
- ⁵³*School of Physics and Astronomy, University of Glasgow, Glasgow, United Kingdom*
- ⁵⁴*Oliver Lodge Laboratory, University of Liverpool, Liverpool, United Kingdom*
- ⁵⁵*Imperial College London, London, United Kingdom*
- ⁵⁶*Department of Physics and Astronomy, University of Manchester, Manchester, United Kingdom*
- ⁵⁷*Department of Physics, University of Oxford, Oxford, United Kingdom*
- ⁵⁸*Massachusetts Institute of Technology, Cambridge, Massachusetts, USA*
- ⁵⁹*University of Cincinnati, Cincinnati, Ohio, USA*
- ⁶⁰*University of Maryland, College Park, Maryland, USA*
- ⁶¹*Los Alamos National Laboratory (LANL), Los Alamos, New Mexico, USA*
- ⁶²*Syracuse University, Syracuse, New York, USA*
- ⁶³*School of Physics and Astronomy, Monash University, Melbourne, Australia*
(associated with Institution Department of Physics, University of Warwick, Coventry, United Kingdom)
- ⁶⁴*Pontifícia Universidade Católica do Rio de Janeiro (PUC-Rio), Rio de Janeiro, Brazil*
(associated with Institution Universidade Federal do Rio de Janeiro (UFRJ), Rio de Janeiro, Brazil)
- ⁶⁵*Physics and Micro Electronic College, Hunan University, Changsha City, China*
(associated with Institution Institute of Particle Physics, Central China Normal University, Wuhan, Hubei, China)
- ⁶⁶*Guangdong Provincial Key Laboratory of Nuclear Science, Guangdong-Hong Kong Joint Laboratory of Quantum Matter, Institute of Quantum Matter, South China Normal University, Guangzhou, China*
(associated with Institution Center for High Energy Physics, Tsinghua University, Beijing, China)
- ⁶⁷*School of Physics and Technology, Wuhan University, Wuhan, China*
(associated with Institution Center for High Energy Physics, Tsinghua University, Beijing, China)

⁶⁸*Departamento de Fisica, Universidad Nacional de Colombia, Bogota, Colombia*

(associated with Institution LPNHE, Sorbonne Université, Paris Diderot Sorbonne Paris Cité, CNRS/IN2P3, Paris, France)

⁶⁹*Universität Bonn - Helmholtz-Institut für Strahlen und Kernphysik, Bonn, Germany*

(associated with Institution Physikalisches Institut, Ruprecht-Karls-Universität Heidelberg, Heidelberg, Germany)

⁷⁰*Eotvos Lorand University, Budapest, Hungary*

(associated with Institution European Organization for Nuclear Research (CERN), Geneva, Switzerland)

⁷¹*INFN Sezione di Perugia, Perugia, Italy (associated with Institution INFN Sezione di Ferrara, Ferrara, Italy)*

⁷²*Van Swinderen Institute, University of Groningen, Groningen, Netherlands*

(associated with Institution Nikhef National Institute for Subatomic Physics, Amsterdam, Netherlands)

⁷³*Universiteit Maastricht, Maastricht, Netherlands*

(associated with Institution Nikhef National Institute for Subatomic Physics, Amsterdam, Netherlands)

⁷⁴*DS4DS, La Salle, Universitat Ramon Llull, Barcelona, Spain*

(associated with Institution ICCUB, Universitat de Barcelona, Barcelona, Spain)

⁷⁵*Department of Physics and Astronomy, Uppsala University, Uppsala, Sweden*

(associated with Institution School of Physics and Astronomy, University of Glasgow, Glasgow, United Kingdom)

⁷⁶*University of Michigan, Ann Arbor, Michigan, USA (associated with Institution Syracuse University, Syracuse, New York, USA)*

^aDeceased.

^bAlso at Università di Firenze, Firenze, Italy.

^cAlso at Scuola Normale Superiore, Pisa, Italy.

^dAlso at Università di Ferrara, Ferrara, Italy.

^eAlso at Università di Milano Bicocca, Milano, Italy.

^fAlso at Università di Bologna, Bologna, Italy.

^gAlso at Università di Genova, Genova, Italy.

^hAlso at Universidad Nacional Autónoma de Honduras, Tegucigalpa, Honduras.

ⁱAlso at Università di Bari, Bari, Italy.

^jAlso at Università di Cagliari, Cagliari, Italy.

^kAlso at Università di Roma Tor Vergata, Roma, Italy.

^lAlso at Universidade Federal do Triângulo Mineiro (UFTM), Uberaba-MG, Brazil.

^mAlso at Hangzhou Institute for Advanced Study, UCAS, Hangzhou, China.

ⁿAlso at Università di Siena, Siena, Italy.

^oAlso at Università degli Studi di Milano, Milano, Italy.

^pAlso at Central South U., Changsha, China.

^qAlso at Università di Padova, Padova, Italy.

^rAlso at Università di Perugia, Perugia, Italy.

^sAlso at Excellence Cluster ORIGINS, Munich, Germany.

^tAlso at Università di Pisa, Pisa, Italy.

^uAlso at Università della Basilicata, Potenza, Italy.

^vAlso at Università di Urbino, Urbino, Italy.